Numerical Investigation of the Performance of Twisted and Untwisted Blades for Small Horizontal Axis Wind Turbines

M. E. Abdelaty, Abdellatif ,O.,E. and A. M. Osman

Mechanical Engineering Department, Benha University, Shoubra Faculty of Engineering,108 Shoubra Street, Cairo, Egypt, Tel +20-2-22050175-4111, Fax +20-2-2202336, Email m.eng86@yahoo.com or Osama.abdellatif@feng.bu.edu.eg

Abstract:

The present study deals with the computational analysis of a model of a small horizontal axis wind turbine using CFD Simulation. A three dimensional computational model of the rotor system is created and simulation has been carried out using Realizable K-ε turbulent model. The analysis has been carried out at various wind speeds in the range of 4 m/s to 12 m/s to study the variation of torque, axial thrust and power with wind speed. The effect of the twist of the blade on the performance of wind turbine is studied. The flow field characteristics around blades at a section placed on the mid of blades have also been studied. The results show that the untwisted blades give a better performance than twisted blades for the studied conditions [tip speed ratio =6 and Reynolds number range (16000- 51000)] in terms of power, torque and thrust force and pressure distribution around blades for the range of velocities tested.

Key Words: CFD, Horizontal axis wind turbines, Twisted Blade and Untwisted Blade

Introduction:

Wind is a plentiful resource of energy in comparison with other renewable energy resources. Moreover, unlike the solar energy, Wind energy can be extracted during the whole day. Wind turbine consists of rotor, generator, driven chain and control system. In order to extract the maximum kinetic energy from wind, researchers put many efforts on the design of effective blade geometry [1].The present work is concentrated on small horizontal axis wind turbines with power range of 3-5 kw. The aerodynamics of flow around the wind turbine blades plays an important role. CFD is a popular approach to study the wind turbine aerodynamics. Many researches try to study the effect of twist on wind turbine blades and show the optimum angle of attack which produce the maximum lift force. Sayed.A et al. [2] studied aerodynamic analysis of different wind-turbine-blade profiles using a Computational Fluid Dynamics (CFD) method based on the finite-volume approach for wind conditions. The Angle of attack has a dominant effect on determining the optimum profile. The optimum operating α

should lie between -4^o and 10^o to get the maximum power extracted from the wind. Thumthae et al. [3] determined the Optimal angle of attack for untwisted blade wind turbine by a numerical simulation of horizontal axis wind turbine (HAWT) with untwisted blades The numerical solution was carried out by solving conservation equations in a rotating reference frame wherein the blades and grids were fixed in relation to the rotating frame. The results showed that the power outputs reach maximum at pitch angles: (4.12^o), (5.28^o), (6.66^o) and (8.76^o) for the wind speeds 7.2, 8.0, 9.0 and 10.5 m/s, respectively. By using the 80% span as the basis for design, the finding indicated that the optimal angles of attack were the ones near the maximum lift point. The angles were slightly larger as the speeds become higher. Ramasamy et al. [4] study the rotor performance with untwisted and highly-twisted blades experimentally by measuring torque at low thrust coefficients. The results indicated that untwisted blades showed identical, if not better, performance when compared with the highly-twisted blades.

Governing Equations:

ANSYS-FLUENT numerically solves the governing equations for fluid flow using finite volume methods. Mass transport equation and three-dimensional momentum transport equations are the fundamental governing equations solved in the CFD code [5].

Mass Conservation Equation

The time dependent mass conservation equation for both compressible and incompressible flows,

$$\frac{\partial \cup}{\partial X} + \frac{\partial v}{\partial y} = 0 \qquad (1)$$

Where:

ρ: Density of Fluid, u &v : Velocity components in x and y directions.

Momentum Equation:

The momentum conservation equation, or the Navier-Stokes equations, used in ANSYS- FLUENT,

$$\rho \frac{DU_i}{Dt} = \frac{\partial P}{\partial X_i} + \frac{\partial}{\partial X_i}\left[\mu \left(\frac{\partial U_i}{\partial x_j} + \frac{\partial U_j}{\partial x_i} \right) - \rho \overline{\dot{u_i} \dot{u_j}} \right] \qquad (2)$$

Where:

μ: Molecular viscosity.

GEOMETRY, CASE SETUP AND BOUNDARY CONDITIONS

The selection of wind turbine rotor configuration include selection of airfoil section, design of blades and optimum pitch angle, design of hub and number of blades and shaft design to get finally the optimum performance of rotor. Three bladed configuration offers best balance between the aerodynamic efficiency, noise levels and blade stiffness, this configuration is observed to be the most common and efficient design for HAWT. In the present study, number of blades has been chosen as three. Airfoils commonly used in wind turbine blades are NACA 44xx and NACA 00xx series due to maximum lift coefficients, low pitching moment, and minimum drag. In the present study, NACA 4418 airfoil section has been used. The aerodynamic characteristics of NACA 4418 are zero-lift angle of attack of - 4°, maximum lift to drag ratio or slide ratio (C_L / C_D)max of 44.447 which corresponds to angle of attack of 6.5° and lift coefficient of 1.209 as shown in figure [1].

The tip speed ratio (λ):

$$\lambda = \frac{\omega R}{V} \tag{3}$$

Where:

λ: Tip speed ratio, ω: Angular velocity of rotor , V: Wind speed and R:Radius of rotor.

For electrical power generation (λ) should be greater than 4 so that, the most common value of (λ) of 6 has been chosen based on literature [7]. In order to arrive at the blade configuration blade element momentum (BEM) theory has been used as shown in fig 2. The chord (c) and the angle of relative wind (ϕ_r) of the blade at every section has been found from equations below [8]. All the design parameters are summarized in table 1 according to the following equations:

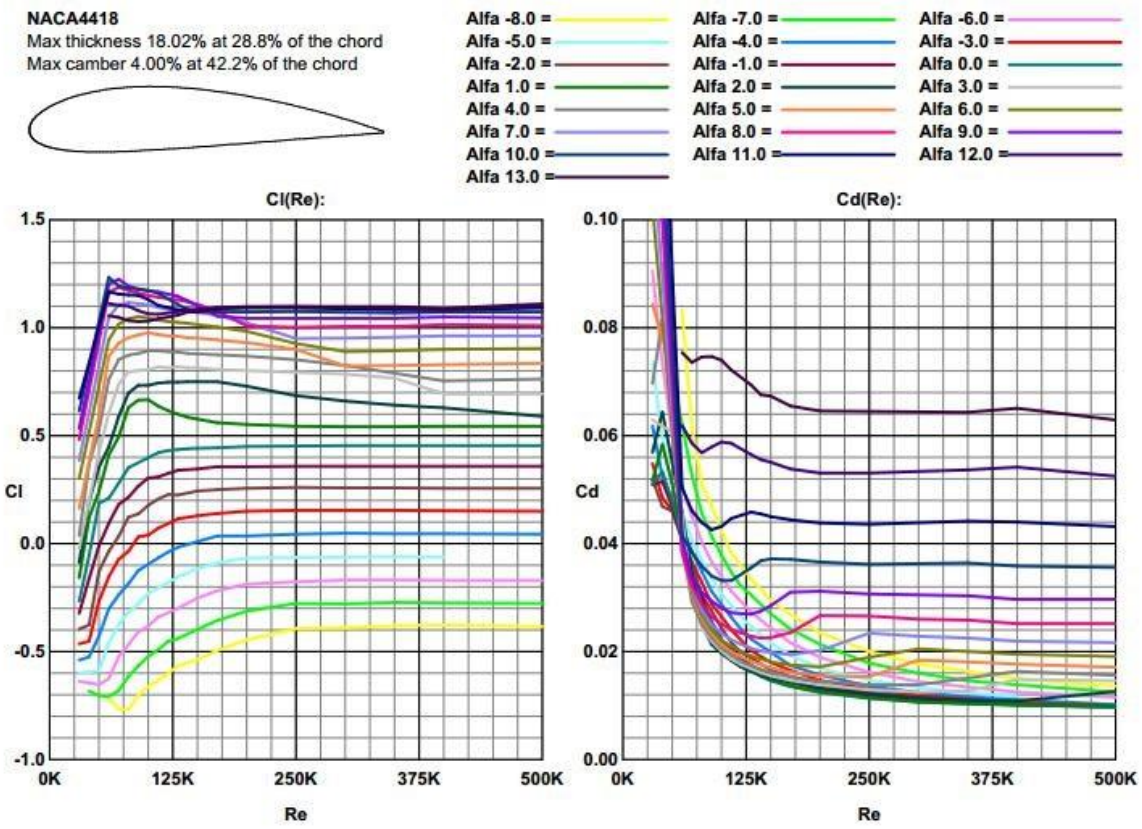

Figure 1: Aerodynamic characteristics of NACA 4418 (C_L & C_d) for different angle of attacks and Reynolds number [6].

$$\phi_r = \frac{2}{3} tan^{-1}\left(\frac{1}{\lambda_r}\right) \quad (4)$$

$$c = \frac{8\pi r}{BC_L} 1 - cos\phi_r \quad (5)$$

$$\lambda_r = \lambda\left(\frac{r}{R}\right) \quad (6)$$

Where:

c: Chord , r : Radial length of the element , C_L :Lift coefficient and ϕ_r :Relative angle of blade with wind direction.

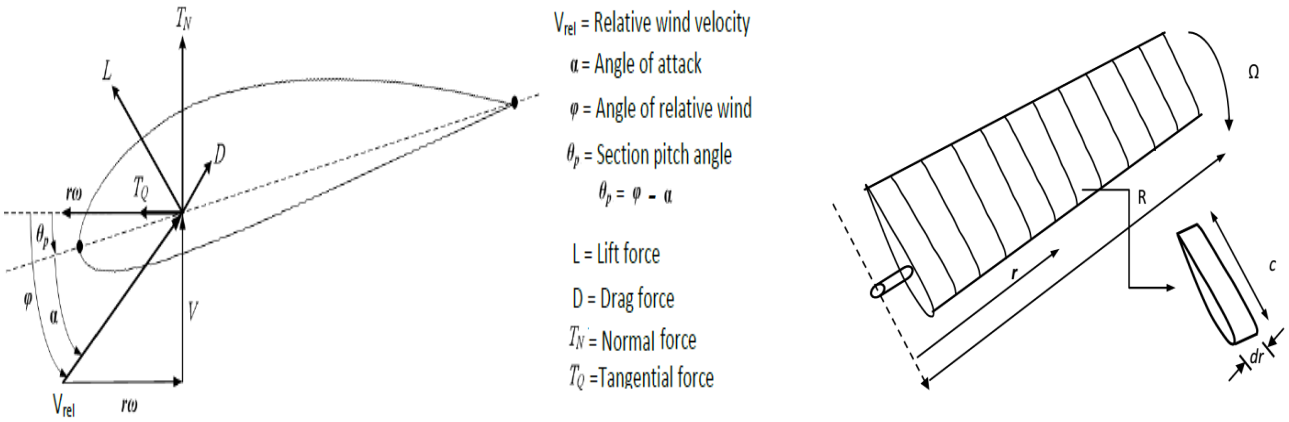

Figure. 2: Schematic representations of blade elements.

Blade twist angle (θ_T):

$$\theta_T = \theta_p - \theta_{p,0} \quad (7)$$

$$\theta_p = \phi_r - \alpha \quad (8)$$

Where:

$\theta_{p:}$ Blade pitch angle.

$\theta_{p,0:}$ Blade pitch angle at the tip

α: Angle of attack.

The chord and twist variations of the blade found from BEM theory are given below in table (1).

For untwisted blade the blade has a maximum chord of (35.872mm) at hub and smallest chord of (9.44 mm) at tip.

The analysis of rotor has been carried out using Moving Reference Frame (MRF) technique which requires the creation of different zones of fluid for treatment in the stationary and moving reference frames. The modeled rotor with twisted blades and untwisted blades are shown in figure (3).

Table (1): Geometry of Twisted blade

S.No	Radius(r)(mm)	λ_r	ϕ_r	Chord (c) (mm)	θ_p	Twist angle (θ_T) (deg)
1	25	0.667	0.655	35.872	31.039955	31.232
2	45	1.200	0.463	32.852	20.037047	20.229
3	65	1.733	0.349	27.130	13.487760	13.680
4	85	2.267	0.277	22.452	9.370629	9.562
5	105	2.800	0.229	18.942	6.602549	6.794
6	125	3.333	0.194	16.299	4.632829	4.825
7	145	3.867	0.169	14.267	3.166778	3.359
8	165	4.400	0.149	12.666	2.036177	2.228
9	185	4.933	0.133	11.377	1.139168	1.331
10	205	5.467	0.121	10.321	0.410882	0.6027
11	225	6.000	0.110	9.440	-0.191785	0.000

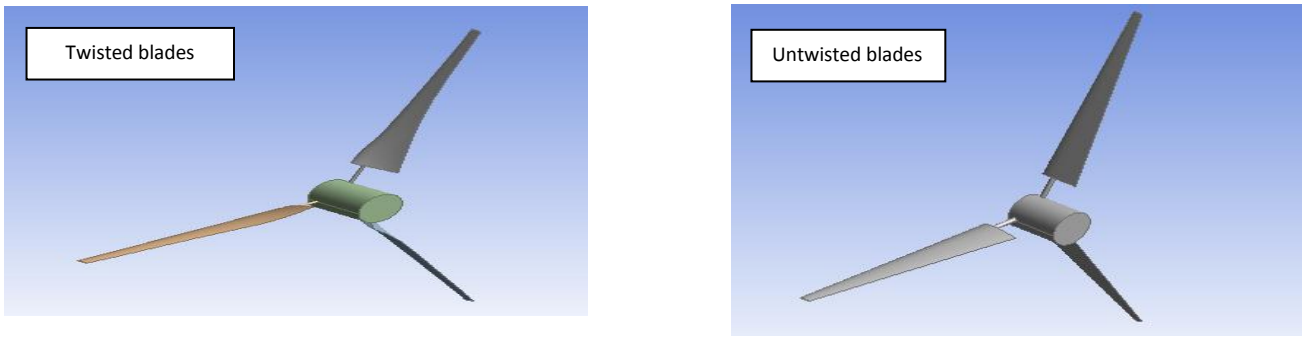

Figure 3: Modeled rotor with twisted and untwisted blades

In this study, the three dimensional computational domain developed in ANSYS 14.5 software as shown in Figure (4) and Figure (5) which also show the fully meshed computational domain. The meshing details and simulation parameters are given in Table (2). Velocity inlet and pressure outlet boundaries have been defined at the upstream face and downstream face of the outer cylinder, respectively. Symmetry boundary condition has been assigned to the curved surface of the outer cylinder. The rotor faces have been assigned wall/no-slip boundary condition. Double precision pressure based solution has been used in the present work to predict good results. Turbulence intensity of 5% has been chosen as the flow has been observed to be fully developed at this level of turbulence intensity [9]. In the pressure outlet, gauge pressure has been set to zero and the same turbulence intensity (5%) and hydraulic diameter as velocity inlet were given to reduce convergence difficulties. The faces of the inner cylinder serve as an interface between stationary and rotating part of the model. The

rotating zone has been selected as the inner cylinder and the moving reference frame option was enabled. Corresponding to the tip speed ratio of 6, the angular velocity has been given for the inner domain fluid. Initial values for various flow variables over the entire computational domain were set equal to the inlet boundary values. The solution is obtained and presents the Torque, Normal force and power produced by the rotor from ANSYS fluent solver.

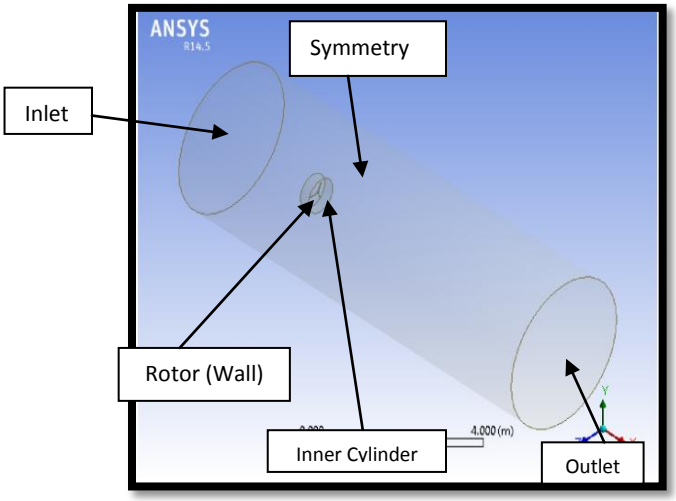

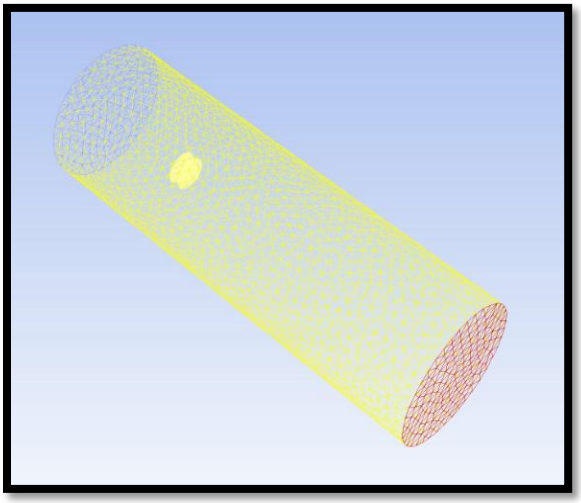

Figure.4: Computational domain with boundary conditions. Figure5: Mesh of Computational domain with rotor.

Table (2): CFD Simulation Parameters:

Mesh	Type A hybrid elements , unstructured grid , No. of grid nodes 338947, No of Element 1814124, No of Faces 3696862	
Turbulence	For K-ε Realizable K-epsilon with Standard wall function with constant TDR=1.2 C_2=1.9 TKE=1	
Material:	air	
Numerical Scheme	Second order accuracy was used. SIMPLE pressure – velocity coupling was used.	
Convergence criteria	less than 1e-6	
Boundary conditions	Inlet : Velocity magnitude :4,6,8,10,12 m/s Turbulence intensity : 5% ,	Outlet : Pressure outlet Turbulence intensity : 5%

Computational process examines whether the physical models used in computer simulations agree with real world observations. The basic validation strategy is to identify and quantify both error and uncertainty through comparison of simulation results with experimental or numerical solution data. ANSYS Fluent code using k-ε turbulent model is used to simulate the rotor blade design results with the results published in [10]. The Power outputs obtained by present CFD simulations are compared with data output reported at different wind speed as shown in Fig. 6. The results show that a good agreement between the present CFD work and published results with acceptable difference.

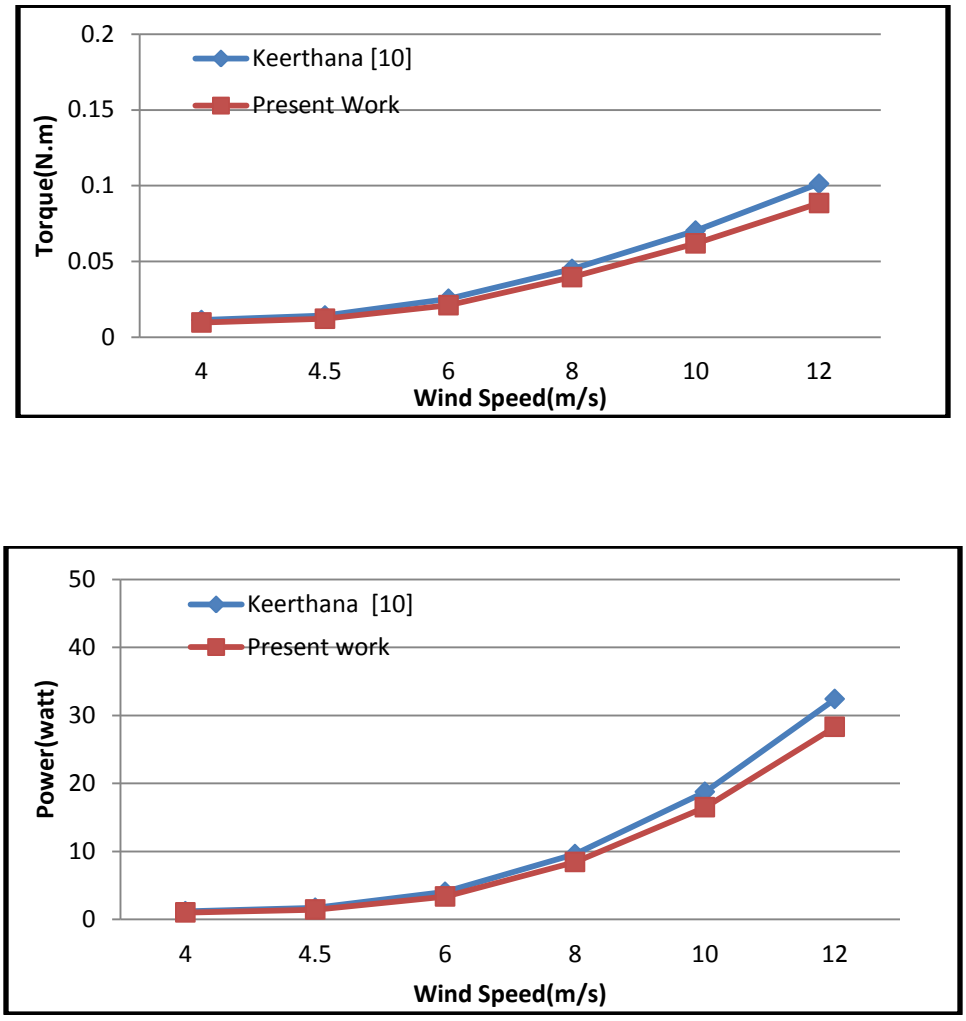

Figure 6: comparison between power output and torque obtained by present CFD simulation and Keerthana [10] simulation with different wind speed.

RESULTS AND DISCUSSION:

The present's comparison of numerical results obtained by twisted and untwisted blades in terms of torque and power of wind turbine rotor using the tip speed ratio of 6 for different wind speeds and the performance parameters are shown in figures (7-9).

Figure[7]shows the variation of torque with wind speed obtained by the untwisted and twisted blades. Both types of blades produce the same amount of torque at wind velocity 4m/s increasing wind velocity up to 6 m/s the untwisted blade get more torque than twisted blade about (8-10%). The difference in torque between twisted and un twisted blade increase with increasing wind velocity and the maximum difference at wind speed 12m/s about (13%) increase in torque.

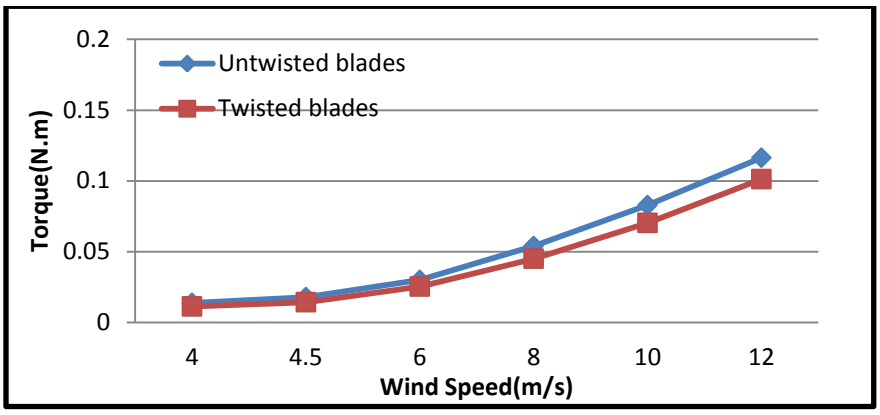

Figure.7: Variation of torque with wind velocity.

Figure [8] shows the variation of power with wind speed obtained by two configurations of rotor. The two configuration of rotor produce the same amount of power at wind velocity (4-6)m/s and untwisted blade produce more power than twisted with increasing wind speed and maximum difference between two configuration at wind speed 12m/s.

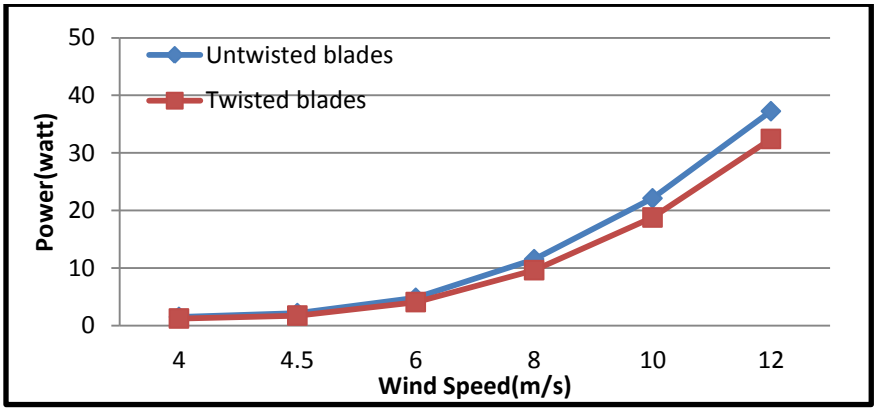

Figure.8: Variation of power with wind velocity.

Figure [9] shows the variation of thrust force with wind speed obtained in both configurations of rotor. The thrust force produce by untwisted and twisted blades approximately have same value at speed 4m/s. Increasing wind speed the thrust force for untwisted increase comparing with twisted blades.

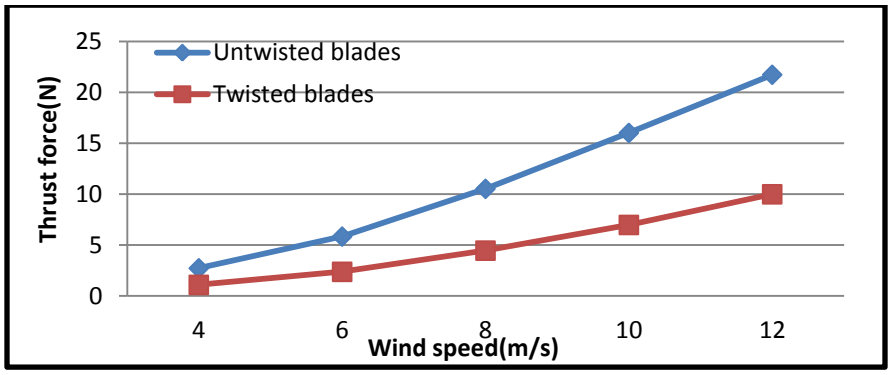

Figure.9: Variation of thrust force with wind speed.

Blade rotation has two main effects on the behavior of the flow. First, it causes the dynamic pressure along the blade to increase towards the tip. Second, it leads to the appearance of two external forces. One of the two forces is in a rotating frame of reference, namely the centrifugal while the other is Coriolis forces. These effects act differently on attached and separated flow and can lead to the so-called stall delay phenomenon. The untwisted and twisted blades are shown as a contours produce the same pressure distribution along the length of blades so the two configuration produce the same power for low wind velocities (4-6 m/s) as shown in figures (10-11). Increasing the wind velocity up to 12m/s the pressure distribution on untwisted blades shows difference in pressure between upper and lower surface of blades near the tip as shown in figures (12-13-14). However untwisted blades produce more torque than twisted blade in the upper limit of wind velocity. The pressure contours around blades for range of velocity tested are shown in figures (10-14).

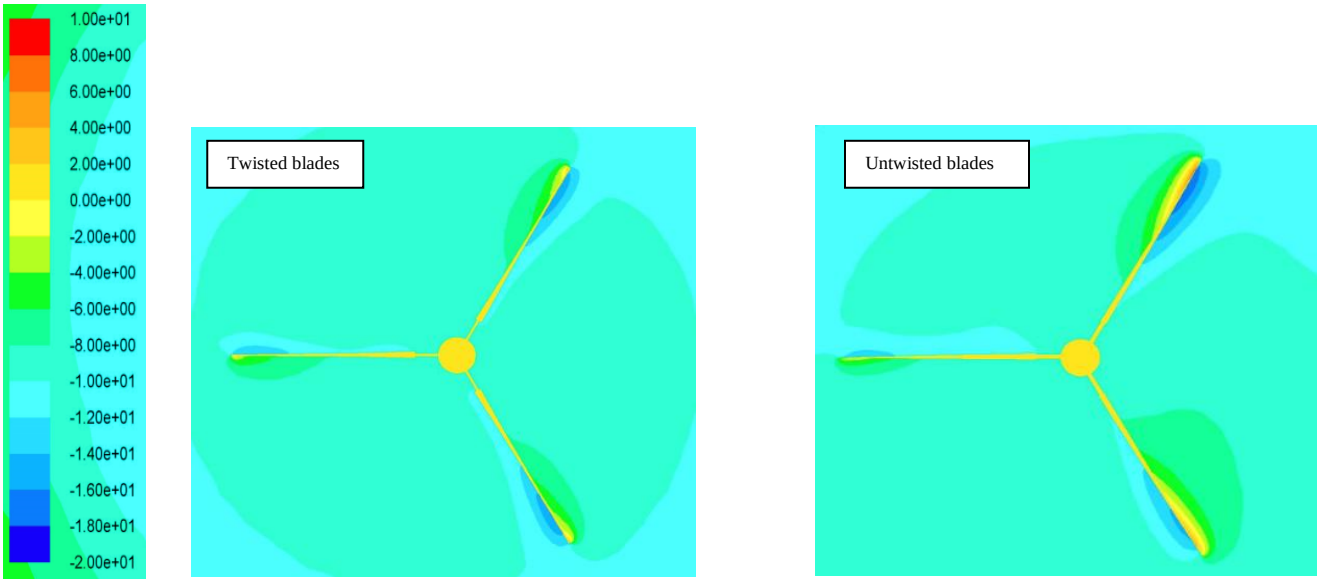

Figure.10: Pressure contour around blades at wind velocity 4m/s.

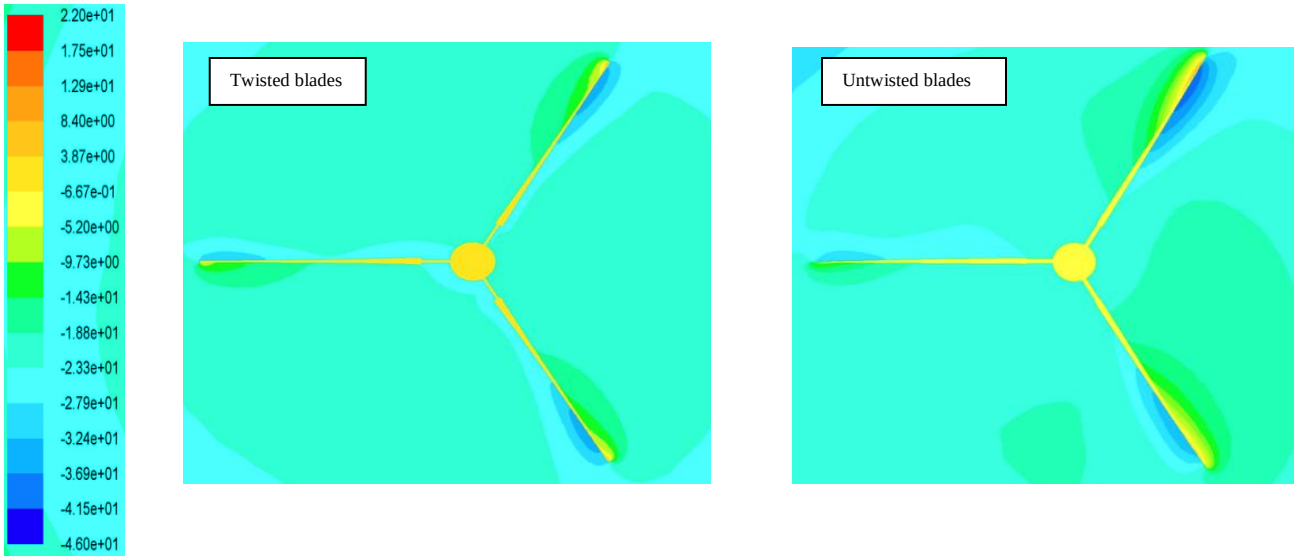

Figure.11: Pressure contour around blades at wind velocity 6m/s.

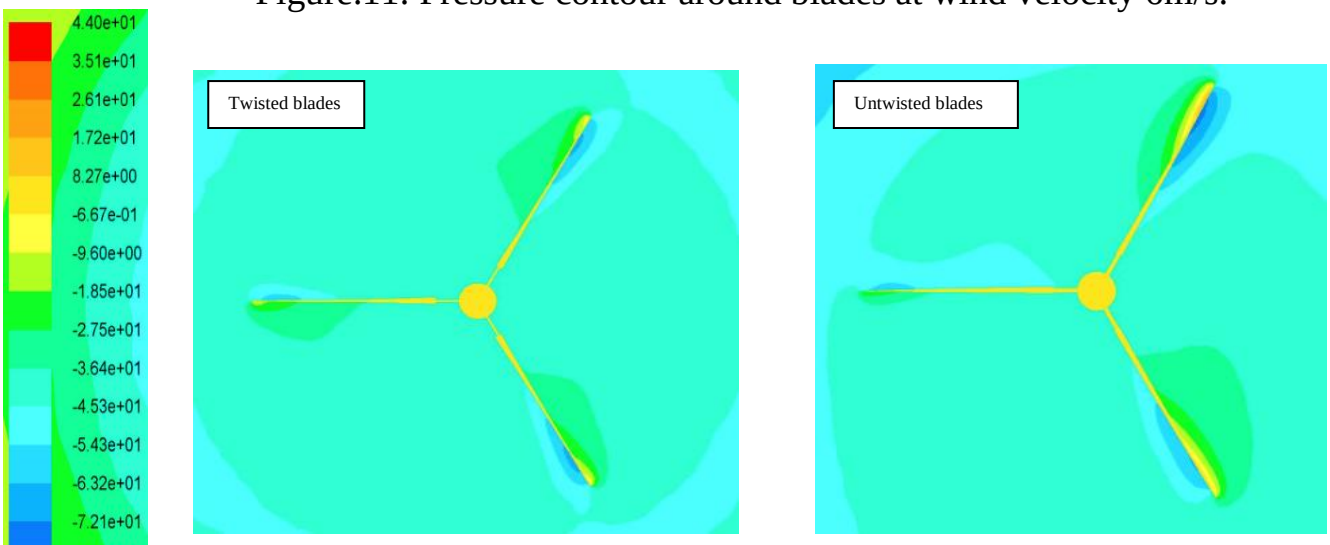

Figure.12: Pressure contour around blades at wind velocity 8m/s.

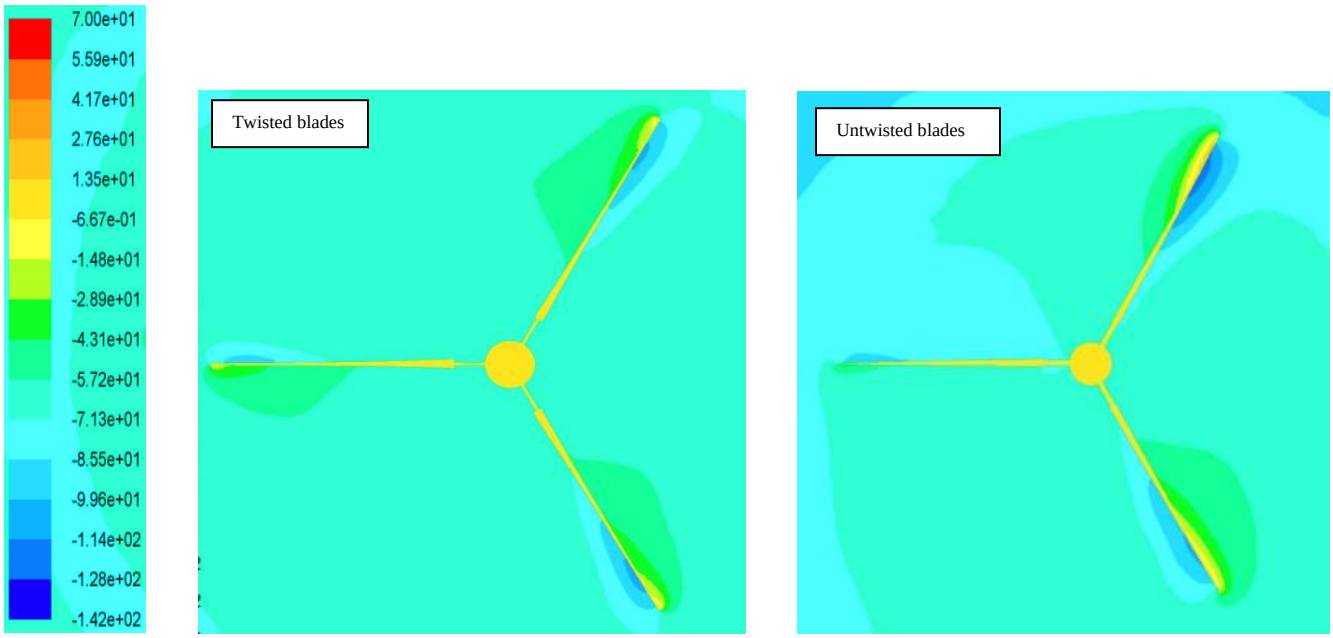

Figure.13: Pressure contour around blades at wind velocity10 m-s.

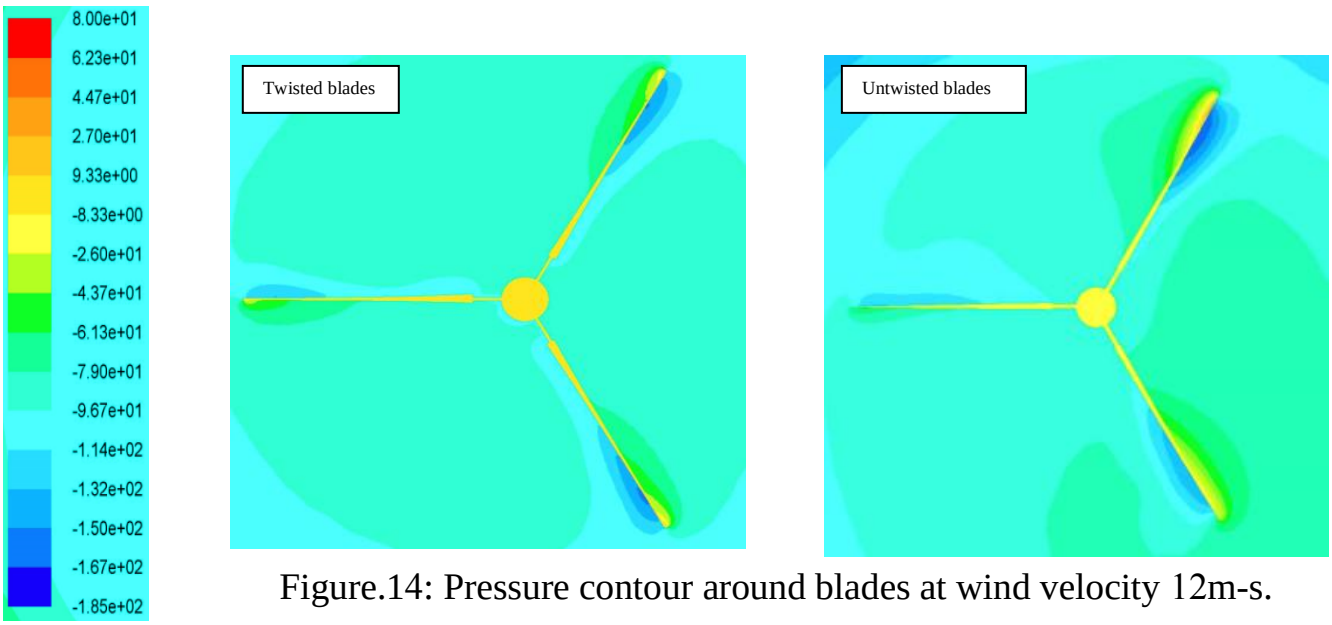

Figure.14: Pressure contour around blades at wind velocity 12m-s.

Conclusion:

CFD simulation has been done to study the performance of wind turbine at various wind speeds in the range of 4 m/s to 12 m/s. Two models of blades, the first is untwisted and the second is twisted one are used. The results indicate that:

The simulation using realizable K-ε model seems to get good results comparing with other models. At low velocities there is small difference in torque produced by untwisted over twisted blade (about 3%).At speeds up to 6 m/s the difference in torque produced by untwisted and twisted blade is noticed and the untwisted blades give better performance than twisted blades at this region of velocities (about 8-10% increase in torque.).The increase in torque with untwisted blades as compared with twisted blades is explained by the pressure distribution obtained by the present CFD results. It should be noted that the thrust force is also increased for untwisted blades as compared with twisted blades. However from the above results the untwisted blades give a better performance than twisted blades in small scale wind turbines in the range investigated.

Abbreviations:

BEM Blade element momentum.
CFD Computational Fluid Dynamics.
HAWT Horizontal axis wind turbine.
TDR Time-domain reflectometry.
TKE Turbulent kinetic energy.
MRF Moving reference frame.
NACA National advisory committee for aeronautics.

Nomenclatures:

B Number of blades.
c Chord.
C_L Lift coefficient.
C_D Drag coefficient.
μ Molecular viscosity.
P Static pressure.
r Radial length of the element.
R Radius of rotor.
V Wind speed.

Greek letters:

α Angle of attack.
λ Tip speed ratio.
ω Angular velocity of rotor.
ϕ_r Relative angle of blade with wind direction.
θ_T Blade twist angle.
θ_p Blade pitch angle.
$\theta_{p,0}$ Blade pitch angle at the tip.

References:

[1] Han.C " Aerodynamics Analysis of Small Horizontal Axis Wind Turbine Blades by Using 2D and 3D CFD Modelling" M.Sc. thesis, University of the Central Lancashire, (2011).

[2] Sayed.A , Kandil,H.,A. and Ahmed Shaltot "Aerodynamic analysis of different wind-turbine-blade profiles using finite-volume method Energy Conversion and Management" (2012).

[3] Chalothorn.T and Chitsomboon.T "Optimal angle of attack for untwisted blade wind turbine"Renewable Energy (2009).

[4] Manikandan.R, Nili.P and Bhagwat.M "Rotor Hover Performance and Flow field Measurements with Untwisted and Highly-twisted Blades" 36th European Rotorcraft Forum, Paris, France, (2010).

[5] FLUENT 14.5 , (2006), User's Guide, ANSYS Fluent Inc, Lebanon, USA.

[6] http://www.profili2.com.

[7] Burton, David Sharpe, Nick Kenkins and Ervin Bossanyi,. 2001 Wind Energy Handbook. Chichester: John Wiley & Sons Ltd.

[8] Man well, J.F, McGowan, J.G, and Rogers, A.L, "Wind Energy Explained: Theory, Design and Application." Second Edition, John Wiley & Sons Ltd, United Kingdom(2009).

[9] Mukhund, P.R, "Wind and Solar Power systems-Design, Analysis and Operation." Taylor & Francis, USA(2009).

[10] Keerthana , Sriramkrishnan.M, Velayutham.T, Abraham.A, Selvi Rajan.S and Parammasivam.K.M "Aerodynamics analysis of a small horizontal axis wind turbine using CFD" National Conference on Wind Engineering (2012).